

# Glass transition and alpha-relaxation dynamics of thin films of labeled polystyrene

Rodney D. Priestley, Linda J. Broadbelt, and John M. Torkelson\*

*Department of Chemical and Biological Engineering Northwestern University, Evanston, IL 60208-3120, USA*

Koji Fukao†

*Department of Macromolecular Science and Engineering,  
Kyoto Institute of Technology, Matsugasaki, Kyoto 606-8585, Japan*

(Dated: February 14, 2013)

The glass transition temperature and relaxation dynamics of the segmental motions of thin films of polystyrene labeled with a dye, 4-[N-ethyl-N-(hydroxyethyl)]amino-4-nitroazobenzene (Disperse Red 1, DR1) are investigated using dielectric measurements. The dielectric relaxation strength of the DR1-labeled polystyrene is approximately 65 times larger than that of the unlabeled polystyrene above the glass transition, while there is almost no difference between them below the glass transition. The glass transition temperature of the DR1-labeled polystyrene can be determined as a crossover temperature at which the temperature coefficient of the electric capacitance changes from the value of the glassy state to that of the liquid state. The glass transition temperature of the DR1-labeled polystyrene decreases with decreasing film thickness in a reasonably similar manner to that of the unlabeled polystyrene thin films. The dielectric relaxation spectrum of the DR1-labeled polystyrene is also investigated. As thickness decreases, the  $\alpha$ -relaxation time becomes smaller and the distribution of the  $\alpha$ -relaxation times becomes broader. These results show that thin films of DR1-labeled polystyrene are a suitable system for investigating confinement effects of the glass transition dynamics using dielectric relaxation spectroscopy.

PACS numbers: 71.55.Jv; 81.05.Lg; 77.22.Ch

## I. INTRODUCTION

In recent years, intensive studies on the dynamics and the glass transition in confined systems have been undertaken to elucidate the nature of the glass transition [1, 2]. The most promising scenario for the mechanism of the glass transition is based on the Adam-Gibbs theory, in which a length scale characteristic of the dynamics associated with structural relaxation increases with decreasing temperature from the liquid state to the glassy state [3]. A major motivation for studies on the glass transition in a confined geometry was to measure the characteristic length scale directly using different experimental techniques [4, 5].

Polymer thin films are one of the ideal confined systems for such investigations because the system size, i.e., film thickness, can be easily controlled experimentally. For this reason, many investigations were conducted on thin polymer films with various film thickness to measure the glass transition temperature ( $T_g$ ) and the dynamics of the  $\alpha$ -process, which corresponds to the structural relaxation and is related to the cooperative segmental motion of polymer chains. For thin films supported on a substrate, many experimental results show that  $T_g$  decreases with decreasing film thickness if there is no strong attractive interaction, although there have been some conflicting experimental results [6, 7, 8, 9, 10, 11, 12]. In particular, a very large decrease in  $T_g$  has been reported in freely-

standing films of polystyrene (PS) [13, 14].

The dynamics of thin polymer films have been investigated by many experimental methods such as dynamic light scattering [15], dielectric relaxation spectroscopy [16, 17, 18, 19, 20], dynamic mechanical measurement [21], second harmonic generation (SHG) [22], and so on. In accordance with the decrease in  $T_g$ , the dynamics of the  $\alpha$ -process, which are directly associated with the glass transition, become faster with decreasing film thickness. In previous studies by Fukao et al., dielectric relaxation spectroscopy was applied to the investigation of the dynamics of ultrathin polymer films and provided much information about the relaxation dynamics of the  $\alpha$ -process, the  $\beta$ -process and the normal mode in the case of polystyrene [16, 17, 23], poly(vinyl acetate) [24], poly(methyl methacrylate) [24, 25], and cis-poly(isoprene) [25]. Although the glass transition and dynamics of thin films of polystyrene have been investigated intensively, it is very difficult to obtain the dielectric loss signal of the  $\alpha$ -process due to the very low polarity of polystyrene.

The above studies on the dynamics of thin polymer films are mainly related to the average  $T_g$  and the average relaxation time of the  $\alpha$ -process. However, it has been expected that there is a distribution or a positional dependence of  $T_g$  and the relaxation time of the  $\alpha$ -process within polymer thin films, especially thin supported films. Ellison and Torkelson prepared multilayer films of labeled and unlabeled polystyrene and successfully showed that there is a large difference in  $T_g$  between the regions near the free surface and near the substrate using fluorescence measurements [26]. The  $T_g$  of a 14-nm-thick layer at the free surface is 32 K lower than the

\*Corresponding author: j-torkelson@northwestern.edu

†Corresponding author: kfukao@se.ritsumei.ac.jp

bulk  $T_g$ , while  $T_g$  near the substrate is equal to the bulk  $T_g$ . It may be expected that analogous studies involving dielectric measurements of multilayer polystyrene films can reveal the distributions of the dynamics within thin film layers, which are consistent with the distribution of  $T_g$ . However, such studies have not been previously conducted because no one had developed a system in which only one layer of a multilayer film is dielectrically active.

As for the use of guest dipoles to enhance the dielectric response of a weak polar material, there are several reports in the literature [27, 28, 29, 30, 31, 32, 33]. Thus, it has been previously established that the incorporation of guest dipoles into a non-polar polymer is a useful method to enhance its dielectric strength. In this study, we investigate the dielectric properties of single layer films of polystyrene labeled with a nonlinear optical dye DR1 with various film thicknesses and compare them with those previously observed for unlabeled polystyrene in order to discuss the possibility of position-dependent measurements of the dynamics of the  $\alpha$ -process for a multilayer film. It should be noted that this work is the first study to investigate the impact of confinement using dielectric relaxation spectroscopy of a labeled polymer.

This paper consists of six sections. After giving experimental details in Sec. II, the glass transition temperature of thin films of PS labeled with DR1 is shown in Sec. III. In Sec. IV, experimental results on the dielectric relaxation of the  $\alpha$ -process of thin films of PS labeled with DR1 are given. After discussing the experimental results in Sec. V, a summary of this paper is given in Sec. VI.

## II. EXPERIMENTS

In the present study, we use polystyrene labeled at a low level with a nonlinear optical dye, 4-[N-ethyl-N-(hydroxyethyl)amino-4-nitrazobenzene (Disperse Red 1, DR1) (Fig. 1), which we refer to as PS-DR1. The PS-DR1 is a random copolymer of neat styrene monomer and DR1-labeled monomer synthesized following a procedure outlined in Ref. [34]. Hence, the dye molecules DR1 are covalently attached to the polymer chains of polystyrene. The concentration of DR1 in PS-DR1 is approximately 3.0 mol % and  $M_w=1.34\times 10^4$  g/mol and  $M_w/M_n=1.65$ . The molecular dipole moment of DR1 is approximately 7.0 D [35]. It has been established that when doped in PS, the DR1 reorientation dynamics measured by SHG are coupled to cooperative segmental dynamics and can be used as a probe of the  $\alpha$ -process [36]. Also, a related study demonstrated that the reorientation dynamics of DR1 labeled to polymers are coupled to the  $\alpha$ -process [34]. The incorporation of DR1 from 0.0 to 3.0 mol % label content to PS results in a linear enhancement of the dielectric response, indicating that dye-dye associations (dipole quenching) do not occur in 3.0 mol% PS-DR1.

Thin polymer films are prepared by spin-coating from a toluene solution of PS-DR1 onto an aluminum(Al)-

deposited glass substrate. Film thickness is controlled by changing the concentration of the solution and spin speed of the spin-coater. The thin films obtained by spin-coating are annealed *in vacuo* for 48 hr at 303 K. After annealing, Al is vacuum-deposited onto the thin films to serve as an upper electrode. Vacuum deposition of Al might increase the temperature of thin polymer films locally. However, no dewetting of the polymer films are observed during the vacuum deposition of Al. Therefore, the local heating of thin polymer films by vacuum deposition, if any, would not affect the present experimental results. The thickness of the Al electrode is controlled to be 40 nm, which is monitored by a quartz oscillator, and the effective area of the electrode  $S$  is 8.0 mm<sup>2</sup>. The thickness  $d$  of PS-DR1 is evaluated from the electric capacitance after calibration with the absolute thickness measured by an atomic force microscope.

Dielectric measurements are performed using an LCR meter (HP4284A) for the frequency range  $f$  from 20 Hz to 1 MHz and an impedance analyzer with a dielectric interface (Solartron Instruments 1260/1296) for the frequency range from 0.1 Hz to 1 MHz. The temperature of a sample cell is changed between 273 K and 413 K at a constant rate of 1 K/min. The dielectric measurements during the heating and cooling processes are performed repeatedly several times. Data acquisition is made during the above cycles except the first cycle. Good reproducibility of dielectric data is obtained after the first cycle.

As shown in a previous study [17], the resistance of the Al electrodes cannot be neglected for dielectric measurements of very thin films. This resistance leads to an artifact loss peak on the high frequency side. Because the peak shape in the frequency domain is described by a Debye-type equation, the ‘‘C-R peak’’ can easily be subtracted. Thus, the corrected data are used for further analysis in the frequency domain.

## III. GLASS TRANSITION TEMPERATURE OF THIN FILMS OF PS LABELED WITH DR1

Figure 1 shows the real and imaginary components of the complex dielectric constant observed during the cooling process at the frequency of the applied electric field  $f = 100$  Hz for PS-DR1 and unlabeled PS films. The thicknesses of the PS-DR1 and the unlabeled PS films are 360 nm and 298 nm, respectively, and hence both can be regarded as bulk systems. It is clear that below  $T_g$  there is almost no difference in  $\epsilon'$  and  $\epsilon''$  between the PS-DR1 and the unlabeled PS. However, the values of  $\epsilon'$  and  $\epsilon''$  above  $T_g$  of PS-DR1 are much more enhanced compared to those of the unlabeled PS. As shown in Fig. 1(b), the peak height of the dielectric loss due to the  $\alpha$ -process of PS-DR1 is approximately 65 times larger than that of the unlabeled PS.

Figure 2 shows the temperature dependence of the real part of the complex electric capacitance ( $C'$ ) normalized

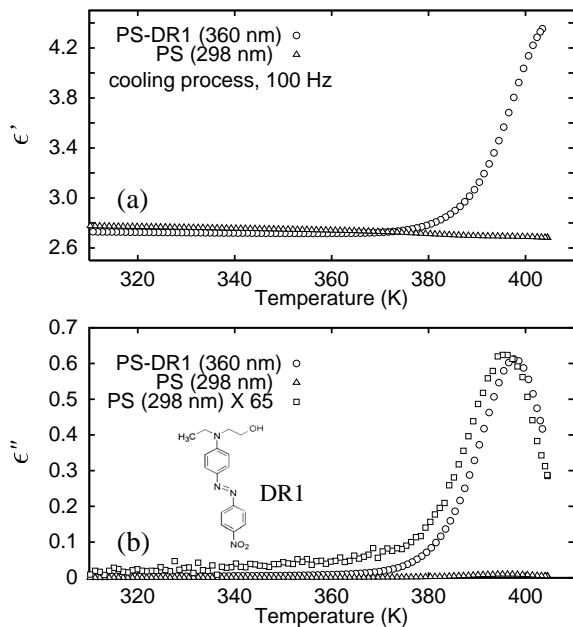


FIG. 1: Temperature dependence of the real and imaginary parts of the complex dielectric constants,  $\epsilon'$  and  $\epsilon''$ , for PS-DR1 ( $d = 360$  nm) and unlabeled PS ( $d = 298$  nm). The data points in this figure are obtained at  $f = 100$  Hz during the cooling process. In Fig. 1(b), the values of  $\epsilon''$  for the unlabeled PS magnified by 65 times are also plotted with square symbols for comparison.

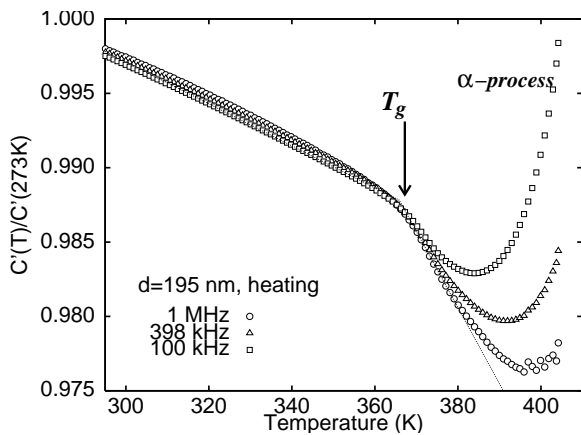


FIG. 2: Temperature dependence of the real part of the electric capacitance normalized by the value at 273 K for thin films of PS-DR1 with  $d = 195$  nm for three different frequencies 100 kHz, 398 kHz, and 1 MHz. These data are observed during the heating process.

to the value at 273 K for three different frequencies. The data are observed during the heating process. From this figure, it is observed that the normalized electric capacitances of the three different frequencies overlap and have a linear temperature dependence below about 368 K. On the other hand, above this temperature the electric capacitance has a linear temperature dependence with a

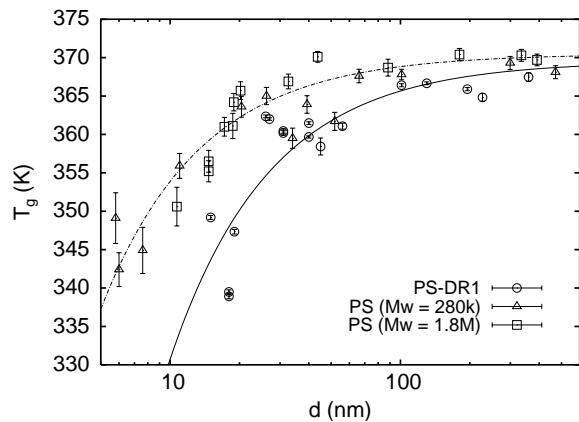


FIG. 3: Thickness dependence of  $T_g$  determined from the crossover temperature as shown in Fig. 2 for thin films of PS-DR1. The thickness dependence of  $T_g$  of the unlabeled PS with  $M_w = 2.8 \times 10^5$  and  $1.8 \times 10^6$  g/mol is also plotted [16, 17]. The solid and dashed curves are obtained by fitting the observed data points to Eq. (1) in the text.

larger slope but has a strong frequency dependence at even higher temperatures. As a result, the electric capacitance deviates from the common straight line. As previously discussed, the negative slope of the straight line  $\tilde{\alpha}$  corresponds to the thermal expansion coefficient normal to the film surface  $\alpha_n$  [16, 17]. If the lateral size of the sample does not change, we have the following relation  $\tilde{\alpha} \approx 2\alpha_n$ . Judging from the electric capacitance in Fig. 1, the value of  $\alpha_n$  increases drastically at 368 K. Therefore, this temperature can be regarded as the  $T_g$  of PS-DR1 with  $d = 195$  nm. The linear thermal expansion coefficient  $\alpha_n$  evaluated from Fig. 2 changes from  $0.7 \times 10^{-4} \text{ K}^{-1}$  to  $2.5 \times 10^{-4} \text{ K}^{-1}$ , which agrees well with the literature values of PS. The frequency dispersion of  $C'$  above  $T_g$  is due to the  $\alpha$ -relaxation process.

Figure 3 shows the thickness dependence of  $T_g$  determined from the temperature dependence of the electric capacitance as mentioned above. This figure clearly shows that  $T_g$  decreases with decreasing film thickness. The thickness dependence of  $T_g$  can be fitted using the following equation:

$$T_g(d) = T_g^\infty \left(1 - \frac{a}{d}\right), \quad (1)$$

where the best fit parameters are  $T_g^\infty = 369.5 \pm 2.1$  K and  $a = 1.1 \pm 0.2$  nm. In Fig. 3 the thickness dependence of  $T_g$  of unlabeled PS is also shown. The molecular weights of the unlabeled PS are  $M_w = 2.8 \times 10^5$  and  $1.8 \times 10^6$  g/mol. The values of  $T_g$  of the unlabeled PS are determined using the same method as previously reported [16]. Comparing the thickness dependence of  $T_g$  between the PS-DR1 and the unlabeled PS, it is found that in both cases  $T_g$  decreases with decreasing film thickness in a reasonably similar way. At the same time, we notice that there is a small difference between the two cases. This difference may be attributed to the difference in molecular weight between the PS-DR1 and the

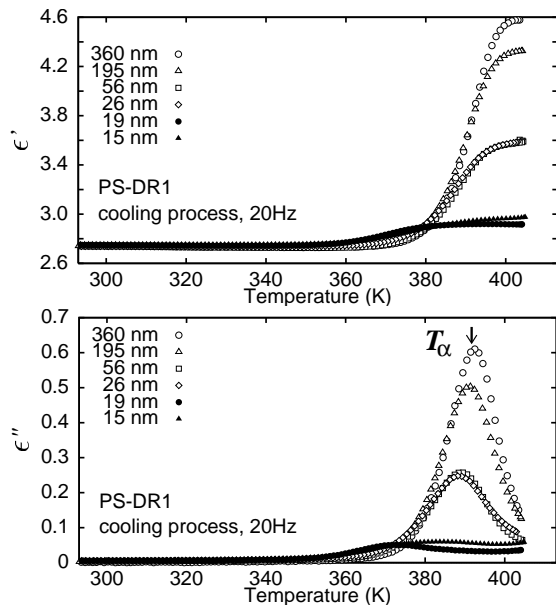


FIG. 4: Temperature dependence of the real and imaginary components of the dielectric constants  $\epsilon'$  and  $\epsilon''$  at the frequency 20 Hz for different film thicknesses.

unlabeled PS, because the molecular weight of PS-DR1 ( $M_w = 1.34 \times 10^4$ ) is much smaller than that of the unlabeled PS, and accordingly  $T_g$  of the bulk state of PS-DR1 is lower by a few degrees than that corresponding to the unlabeled PS. If we take into account the difference coming from the molecular weight, we can judge that the thickness dependence of  $T_g$  of PS-DR1 is fairly comparable to that of the unlabeled PS.

The use of dielectric spectroscopy requires that an upper electrode be evaporated on top of the free surface of the films. A consequence is that the films do not have a true free surface. However, the PS films report a reduction in  $T_g$  with decreasing film thickness similar to techniques that allow for a free surface. Therefore, it is believed that the free surface effects are not masked by the addition of the top electrode as demonstrated previously [16, 18, 20].

#### IV. DYNAMICS OF THE $\alpha$ -PROCESS IN THIN FILMS OF PS LABELED WITH DR1

##### A. Dielectric behavior at a fixed frequency

Figure 4 shows the temperature dependence of the real and imaginary components of the complex dielectric constant for thin films of PS-DR1 with film thickness ranging from 360 nm to 15 nm. The data are obtained during the cooling process at frequency 20 Hz. In Fig. 4 we find that the contribution from the  $\alpha$ -process is strongly affected by film thickness. As the thickness decreases, the peak height of the dielectric loss due to the  $\alpha$ -process becomes smaller, and at the same time the  $\alpha$ -temperature ( $T_\alpha$ )

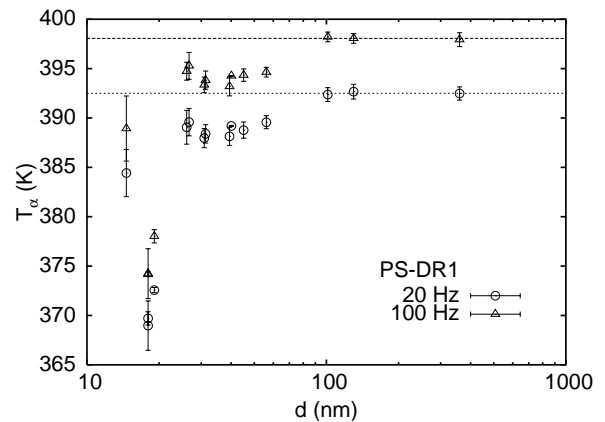


FIG. 5: Thickness dependence of the temperature  $T_\alpha$  observed at 20 Hz and 100 Hz. The dotted and dashed lines correspond to the values observed in bulk states at 20 Hz and 100 Hz, respectively.

at which the dielectric loss due to the  $\alpha$ -process has a maximum is shifted to the lower temperature side. In Fig. 5,  $T_\alpha$  is plotted as a function of film thickness for  $f = 20$  Hz and 100 Hz. The temperature  $T_\alpha$  is found to depend strongly on frequency and to increase with increasing frequency. The value of  $T_\alpha$  at a low frequency corresponding to the  $\alpha$ -relaxation time of 100 sec is comparable to the value of  $T_g$  determined for the ramping process at a rate of 10 K/min using dilatometric measurements or differential scanning calorimetry. Therefore, the decrease in  $T_\alpha$  with decreasing film thickness at a given frequency is associated with the decrease in  $T_g$  and the faster dynamics of the  $\alpha$ -process in thinner films.

##### B. Dielectric relaxation in thin films

Figure 6 shows the frequency dependence of the real and imaginary components of the complex dielectric constants at various temperatures for thin films of PS-DR1 for two different thicknesses: (a)  $d = 360$  nm and (b)  $d = 19$  nm. In the real part of the complex dielectric constant  $\epsilon'$  for the 360nm-thick-film, there is a gradual step from 4.7 to 2.7, while in the imaginary part  $\epsilon''$  there is a maximum at the same frequency where there is the step in  $\epsilon'$ . This frequency dependence is associated with the existence of the  $\alpha$ -process. The peak frequency in  $\epsilon''$  corresponds to the inverse of a characteristic time of the  $\alpha$ -process at a given temperature. From Fig. 6 it is observed that the peak frequency of the  $\alpha$ -process becomes larger with increasing temperature. This corresponds to the acceleration of the dynamics of the  $\alpha$ -process with increasing temperature. At higher temperatures there is also a large increase in  $\epsilon''$  with decreasing frequency. This is usually attributed to the contributions from dc conductivity due to space charges or impurities within the polymeric systems. Comparing the frequency dependences of  $\epsilon'$  and  $\epsilon''$  in Fig. 6(a) to those in Fig. 6(b), we

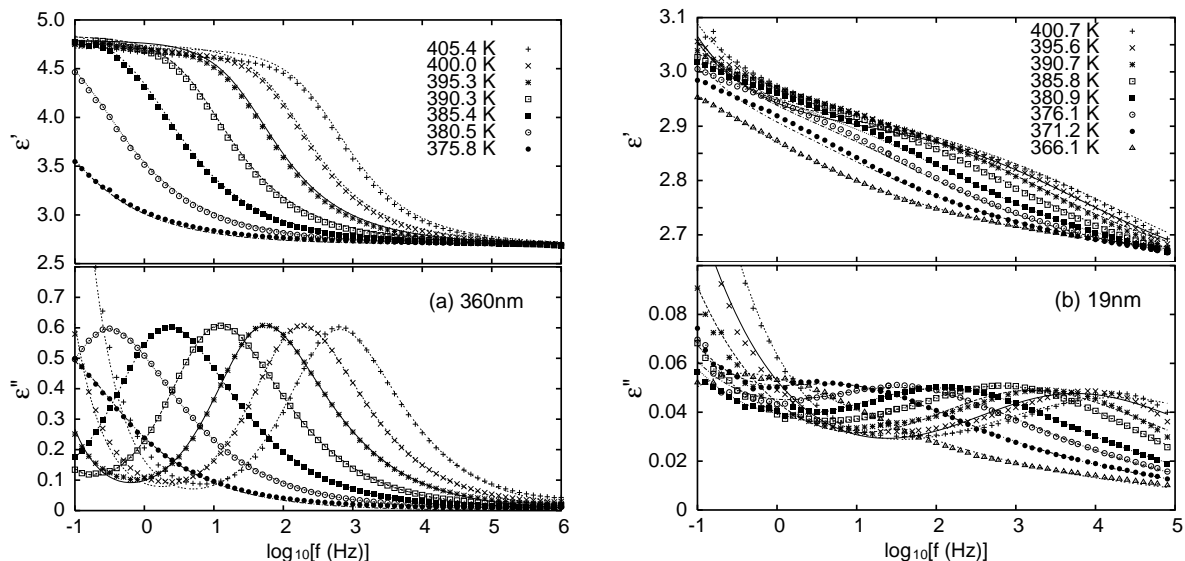


FIG. 6: The dependence of the complex dielectric constant on the logarithm of frequency at various temperatures above  $T_g$  for thin films of PS-DR1: (a)  $d = 360$  nm and (b)  $d = 19$  nm. Solid curves are calculated by Eq. (2).

TABLE I: Fitting parameters of the HN equation for PS-DR1 with various film thicknesses: relaxation strength  $\Delta\epsilon$ , shape parameters  $\alpha_{HN}$ ,  $\beta_{HN}$ , and relaxation time  $\tau_0$ . Here, the exponent  $\beta_{KWW}$  in the KWW relaxation function is evaluated using the relation  $\beta_{KWW} = (\alpha_{HN}\beta_{HN})^{1/1.23}$  [44].

$d$ (nm)	$T$ (K)	$\Delta\epsilon$	$\alpha_{HN}$	$\beta_{HN}$	$\tau_0$ (sec)	$\beta_{KWW}$
19	390.7	$0.33 \pm 0.02$	$0.46 \pm 0.02$	$0.48 \pm 0.10$	$(3.1 \pm 0.5) \times 10^{-4}$	$0.29 \pm 0.06$
26	389.8	$0.96 \pm 0.01$	$0.69 \pm 0.02$	$0.52 \pm 0.02$	$(1.8 \pm 0.1) \times 10^{-2}$	$0.43 \pm 0.24$
360	390.3	$2.14 \pm 0.01$	$0.80 \pm 0.01$	$0.57 \pm 0.01$	$(2.32 \pm 0.04) \times 10^{-2}$	$0.53 \pm 0.08$

TABLE II: The values of the parameters resulting in the best fit of the relaxation times of the  $\alpha$ -process  $\tau$  to Eq. (3) for thin films of PS-DR1 with various film thicknesses ( $d = 360$  nm, 26 nm and 19 nm).

$d$ (nm)	$\log_{10}[\tau_0(\text{sec})]$	$U$ ( $10^3$ K)	$T_0$ (K)	$m$
360	$-11.8 \pm 0.6$	$1.6 \pm 0.2$	$318 \pm 4$	$99 \pm 11$
26	$-13.3 \pm 0.5$	$2.1 \pm 0.2$	$306 \pm 3$	$92 \pm 8$
19	$-14.6 \pm 1.0$	$2.3 \pm 0.4$	$294 \pm 7$	$97 \pm 17$

find that the peak height of the loss peak in  $\epsilon''$  due to the  $\alpha$ -process for  $d = 19$  nm is much smaller than that for  $d = 360$  nm and that the peak shape and the peak position also change with decreasing film thickness.

Here, we use the following empirical equation of  $\epsilon'$  and  $\epsilon''$  as a function of frequency:

$$\epsilon^* = \epsilon_\infty + i \frac{\tilde{\sigma}}{\epsilon_0} \omega^{-m} + \frac{\Delta\epsilon}{[1 + (i\omega\tau_0)^{\alpha_{HN}}]^{\beta_{HN}}}, \quad (2)$$

where  $\omega = 2\pi f$ ,  $\epsilon_0$  is the permittivity *in vacuo* and  $\epsilon_\infty$  is the permittivity at a very high frequency. The second term is a contribution from space charge [37], and this contribution can be attributed to pure dc conductivity if  $m = 1$ . The third term comes from the  $\alpha$ -process, and its empirical form is usually called the Havriliak-Negami (HN) equation, where  $\Delta\epsilon$  is the relaxation strength,  $\alpha_{HN}$

and  $\beta_{HN}$  are the shape parameters, and  $\tau_0$  is the relaxation time of the  $\alpha$ -process. The solid curves in Fig. 6 are obtained using Eq. (2) with the best-fit parameters. In Fig. 6 it is found that Eq. (2) can well reproduce the frequency dependence of the observed dielectric constant. Examples of the best-fit parameters of the HN-equation at 390 K are listed in Table I. In this table, the exponent  $\beta_{KWW}$  is also listed, on the assumption that the relaxation function  $\phi(t)$  is given by the KWW equation  $\phi(t) = \exp(-(t/\tau)^{\beta_{KWW}})$ . The value of  $\beta_{KWW}$  can be evaluated by the relation  $\beta_{KWW} = (\alpha_{HN}\beta_{HN})^{1/1.23}$  and is a measure of the distribution of the relaxation times [44].

### C. Relaxation time of the $\alpha$ -process

Figure 7 shows the Arrhenius plot of the  $\alpha$ -process of thin films of PS-DR1 with  $d = 19$  nm, 26 nm, and 360 nm. The vertical axis is the logarithm of  $1/2\pi\tau$ , where  $\tau$  is the relaxation time of the  $\alpha$ -process and is evaluated from the relation  $2\pi f_{\text{max}}\tau = 1$ , where  $f_{\text{max}}$  is the frequency at which  $\epsilon''$  has a loss peak due to the  $\alpha$ -process at a given temperature. The curves are evaluated using the Vogel-

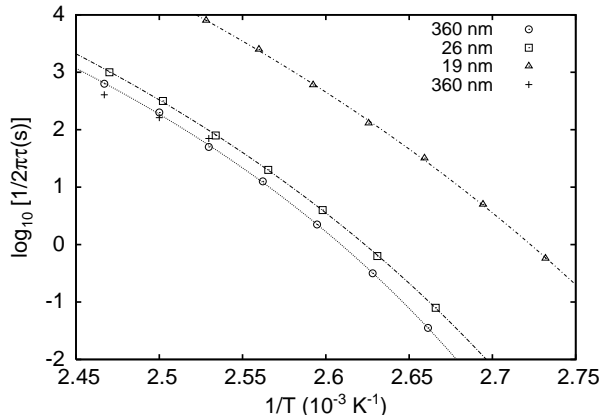


FIG. 7: Arrhenius plot for the  $\alpha$ -relaxation process in thin films of PS-DR1. The logarithm of  $1/2\pi\tau$  vs.  $1/T$  for three different thicknesses  $d = 19$  nm ( $\Delta$ ), 26 nm ( $\square$ ), and 360 nm ( $\circ$ ). The curves are obtained using the VFT law. The symbol  $+$  corresponds to dc-conductivities which are evaluated at 0.1 Hz for  $d = 360$  nm in Fig.10 and are shifted along the vertical axis so that we can compare the temperature dependence of dc-conductivity to that of  $1/\tau$ .

Fulcher-Tammann (VFT) law:

$$\tau(T) = \tilde{\tau}_0 \exp\left(\frac{U}{T - T_0}\right), \quad (3)$$

where  $\tilde{\tau}_0$  is a microscopic time scale for the  $\alpha$ -process,  $U$  is an apparent activation energy, and  $T_0$  is the Vogel temperature [39]. For each film thickness it is found that the relaxation time of the  $\alpha$ -process obeys the VFT law. At the same time, there is a distinct thickness dependence of  $\tau$ , that is, the relaxation time of the  $\alpha$ -process becomes smaller with decreasing film thickness at a given temperature. The best-fit parameters of the VFT law for thin films of PS-DR1 are listed in Table II. It is clear that the Vogel temperature decreases with decreasing film thickness, which is consistent with the fact that  $T_g$  decreases with decreasing film thickness as shown in Fig. 3. The fragility index  $m$ , which is a measure of the non-Arrhenius temperature dependence of the relaxation times, is also evaluated from the temperature dependence of the  $\alpha$ -relaxation time according to the following definition:

$$m = \left[ \frac{d \log_{10} \tau(T)}{d(T_g/T)} \right]_{T=T_g}, \quad (4)$$

where  $T_g$  is defined so that  $\tau(T_g) = 100$  sec [40].

#### D. Profile of the $\alpha$ -loss peak

In order to obtain the thickness dependence of the profile of the dielectric loss spectrum, the observed loss peaks of  $\epsilon''$  at various temperatures are normalized with respect to the peak position for each temperature in the case of

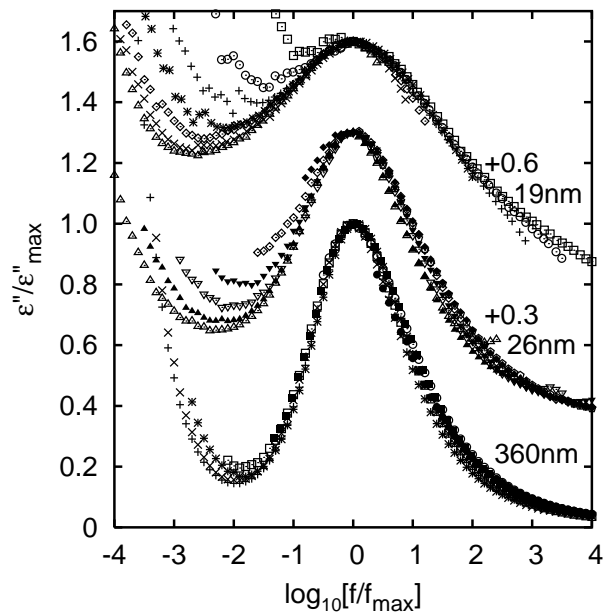


FIG. 8: Dependence of the normalized dielectric loss of PS-DR1 on the logarithm of the normalized frequency. The two axes are normalized with respect to the peak position due to the  $\alpha$ -process, corresponding to  $\epsilon''_{\max}$  and  $f_{\max}$ . The numbers given in the right margin stand for the film thickness. The data for  $d = 19$  nm and 26 nm are shifted up by +0.6 and +0.3, respectively, for clarity. Different symbols correspond to different temperatures: (a) for  $d = 360$  nm, data points at 405.4 K, 400.0 K, 395.3 K, 390.3 K, 385.4 K, 380.5 K, and 375.8 K are plotted (b) for  $d = 26$  nm, 404.9 K, 399.7 K, 394.7 K, 389.8 K, 384.9 K, 380.1 K, and 375.1 K (c) for  $d = 19$  nm, 400.7 K, 395.6 K, 390.7 K, 385.8 K, 380.9 K, 376.1 K, and 371.2 K

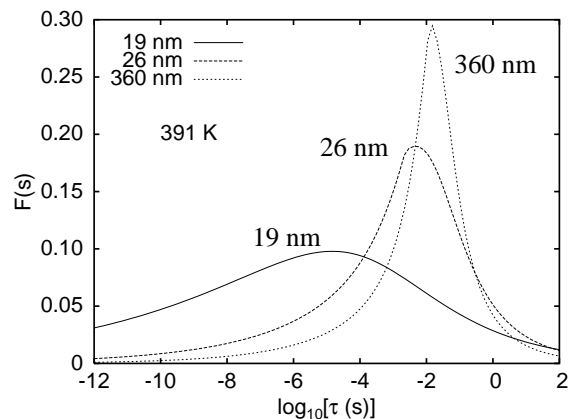


FIG. 9: The distribution function  $F(s)$  of the relaxation times of the  $\alpha$ -process at 391 K for thin films of PS-DR1. The values are calculated by Eq. (6) with the best fit parameters of the HN equation. The dotted curve represents the result for  $d = 360$  nm, the dashed curve that for  $d = 26$  nm, and the solid curve that for  $d = 19$  nm.

three different film thicknesses, as shown in Fig. 8. For clarity, data points of  $d = 19$  nm and  $d = 26$  nm are shifted along the vertical axis by  $+0.6$  and  $+0.3$ , respectively. From Fig. 8 it is found that the width of the  $\alpha$ -loss peak clearly increases with decreasing film thickness. This suggests that the distribution of the relaxation times becomes broader with decreasing film thickness. At the same time, there is a contribution due to the dc conductivity in the low-frequency side, which may disturb the evaluation of the distribution of the relaxation times of the  $\alpha$ -process. In order to avoid this problem, we use the best-fit parameters of the HN equations  $\alpha_{HN}$ ,  $\beta_{HN}$  and  $\tau_0$  and then evaluate the distributions of  $\tau$ .

Here, the distribution function  $F(\log_e \tau)$  of the relaxation times  $\tau$  is defined by the following relation:

$$\epsilon^*(\omega) = \epsilon_\infty + \Delta\epsilon \int_{-\infty}^{+\infty} \frac{F(\log_e \tau) d(\log_e \tau)}{1 + i\omega\tau}. \quad (5)$$

If we assume that the shape of the dielectric loss peak is described by the HN equation, the distribution function  $F(\log_e \tau)$  can be calculated analytically as follows:

$$F(s) = \frac{1}{\pi} [1 + 2e^{\alpha_{HN}(x_0-s)} \cos \pi\alpha_{HN} + e^{2\alpha_{HN}(x_0-s)}]^{-\beta_{HN}/2} \times \sin \left[ \beta_{HN} \tan^{-1} \left( \frac{e^{\alpha_{HN}(x_0-s)} \sin \pi\alpha_{HN}}{1 + e^{\alpha_{HN}(x_0-s)} \cos \pi\alpha_{HN}} \right) \right] \quad (6)$$

where  $s = \log_e \tau$  [24] and  $x_0 = \log_e \tau_0$ . Figure 9 shows the distribution of  $\alpha$ -relaxation times for three different film thicknesses at 391 K, which is evaluated using Eq. (6). It is found that the relaxation time of the  $\alpha$ -process, which is related to the peak position of the distribution, is shifted to a smaller time with decreasing film thickness, and at the same time, the full width at the half maximum of the distribution becomes broader, increasing from 2 decades (for  $d = 360$  nm) to 8 decades (for  $d = 19$  nm).

### E. Conductivity component

Figure 6 shows that there is a contribution of conductivity due to the motion of space charge such as ions included in polymer materials in the low frequency range. In order to analyze this contribution in the low frequency region, we use the second term of the right-hand side of Eq. (2):  $\epsilon''_{\text{con}} \sim \frac{\tilde{\sigma}}{\epsilon_0} \omega^{-m}$ . Making data fit to this equation for various temperatures, we can obtain the temperature dependence of  $\tilde{\sigma}$  and  $m$  for  $d = 19$  nm and 360 nm. It is found that  $m$  is approximately independent of temperature and is equal to  $0.82 \pm 0.02$  for  $d = 360$  nm and  $0.48 \pm 0.01$  for  $d = 19$  nm. If  $\epsilon''_{\text{con}}$  has a  $\omega$  dependence given by  $\omega^{-m}$ , the real part of ac-conductivity  $\sigma'$  is proportional to  $\omega^{1-m}$ . Hence, we obtain the  $\omega$  dependence of  $\sigma$  in the low frequency region as follows:

$$\sigma' \sim \begin{cases} \omega^{0.18} & : d = 360 \text{ nm} \\ \omega^{0.53} & : d = 19 \text{ nm.} \end{cases} \quad (7)$$

In order to extract the dc-conductivity, the dielectric loss  $\epsilon''$  in Fig. 6 are replotted as  $\omega\epsilon_0\epsilon''$  vs.  $\log f$ , where  $\omega\epsilon_0\epsilon''$  corresponds to the real part of conductivity  $\sigma'$ , as shown in Fig. 10. In Fig. 10, it is found that  $\sigma'$  obeys the power-law  $\omega^{1-m}$  in the lower frequency region and tends to approach a constant value with decreasing frequency. This constant value corresponds to the dc-conductivity. For  $d = 360$  nm, the value  $\sigma'$  at 0.1 Hz in Fig. 10 can be regarded as the dc-conductivity because the slope in the low frequency region is small. On the other hand, for  $d = 19$  nm,  $\sigma'$  still decreases with decreasing frequency in the low frequency region around 0.1 Hz, and hence it is impossible to evaluate the dc-conductivity from the present data for  $d = 19$  nm. The dc-conductivities obtained thus for  $d = 360$  nm are plotted in Fig. 6 after shifting them along the vertical axis so that we can compare the temperature dependence of dc-conductivity to that of  $1/\tau$ . In Fig. 6 it found that there is a fairly good agreement between the two data. Therefore, the present results are consistent with previous results that dc-conductivity has a similar temperature dependence of the segmental motion [41]. For detailed comparison, the data at much lower frequencies are highly required.

## V. DISCUSSION

In 1994, Torkelson and coworkers investigated the rotational dynamics of DR1 doped at 2 wt.% in polystyrene using SHG and dielectric relaxation spectroscopy [36]. They found that both SHG and dielectric relaxation spectroscopy yielded almost the same average time constant  $\langle \tau \rangle$ , and that above  $T_g$  the values of  $\langle \tau \rangle$  fit well to the Williams-Landel-Ferry (WLF) equation with appropriate WLF constants [42], which indicated that the rotational reorientation dynamics of DR1 are coupled to the  $\alpha$ -relaxation process of PS.

As shown in the previous section, the dielectric loss peak can be observed above  $T_g$  using dielectric relaxation spectroscopy for thin films of PS-DR1. In our measurement, we observe a very large dielectric loss above  $T_g$  compared to the unlabeled PS. In PS-DR1, DR1 chromophores are attached covalently to the main polymer chain, while DR1 dyes were doped in PS in Ref. [36]. Although there are covalent bonds between DR1 and PS in the present case, the rotational reorientation relaxation times of the labeled DR1 can still be described by the VFT law, which is the same as the WLF equation, as shown in Fig. 7. This is consistent with results in Ref. [36]. Therefore, the rotational reorientation dynamics of DR1 chromophores attached to the polymer main chain, which must be the microscopic origin of the dielectric loss observed in the present study, are equivalent to the cooperative segmental motions of PS, that is, the  $\alpha$ -relaxation process.

Above  $T_g$ , the reorientation dynamics of DR1 coupled with the  $\alpha$ -process have a very large contribution to the dielectric susceptibility, as shown in Fig. 1. In many poly-

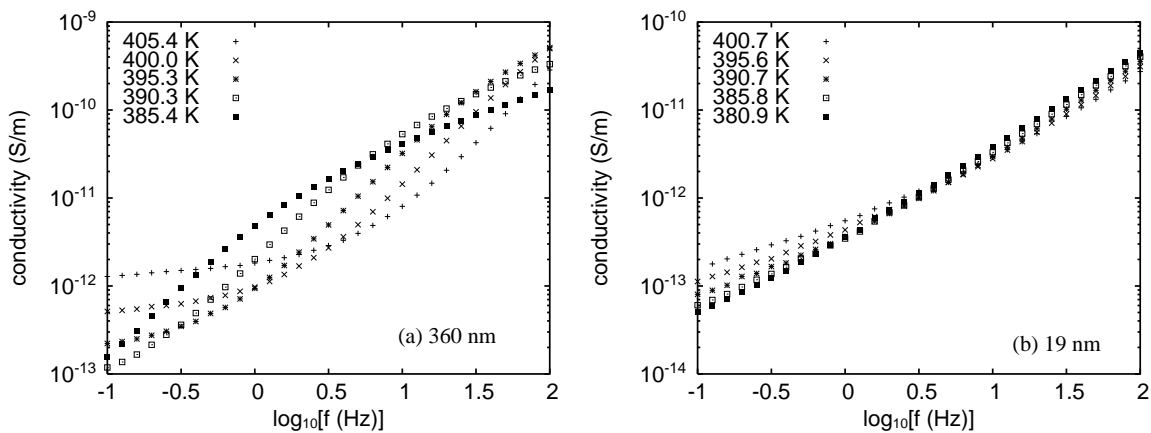


FIG. 10: The frequency dependence of the real part of the conductivity at various temperatures for PS-DR1 with  $d = 360$  nm (a) and  $19$  nm (b). The value of the vertical axis is evaluated from the frequency dependence of the imaginary part of the dielectric ac-susceptibility using the relation  $\sigma' = \omega \epsilon_0 \epsilon''$ .

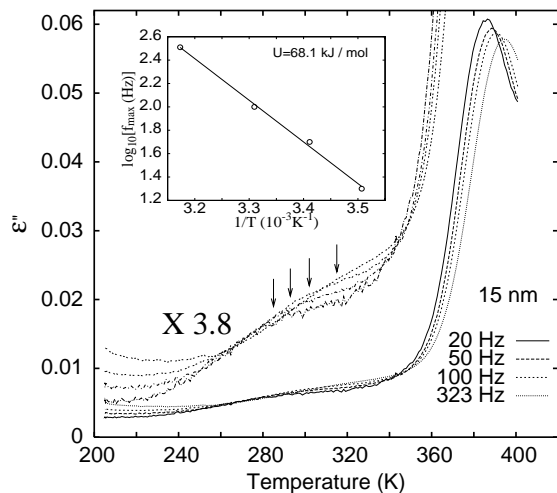


FIG. 11: The dielectric loss as a function of temperature for different frequencies  $20$  Hz,  $50$  Hz,  $100$  Hz and  $323$  Hz for thin films of PS-DR1 with  $d = 15$  nm. The data below  $360$  K are magnified by  $3.8$  times. The arrows indicate the location of the  $\alpha_I$ -process. The inset shows the Arrhenius plot for the  $\alpha_I$ -process.

meric systems with large polarity such as PMMA and PVAc, it is impossible to determine  $T_g$  using capacitive dilatometry [17, 43]. However, as shown in Fig. 2,  $T_g$  can be successfully determined by capacitive dilatometry in the case of PS-DR1. Furthermore, the thickness dependence of  $T_g$  in thin films of PS-DR1 can also be determined and is found to be consistent with that of unlabeled PS. From this result we can conclude that the rotational reorientation dynamics of DR1 are an excellent sensor for the  $\alpha$ -process in thin films of PS, and the results obtained in thin films of PS-DR1 can be compared with those of unlabeled PS.

From Fig. 3 it is observed that  $T_g$  decreases with de-

creasing film thickness for PS-DR1 in a similar manner as unlabeled PS. The reduction in  $T_g$  with decreasing film thickness is believed to be related to a layer at the upper Al-electrode polymer interface with a reduced  $T_g$ . Thus, with decreasing polymer film thickness, the layer with a reduced  $T_g$  contributes more to the average dynamics of the film, leading to a decrease in the average film  $T_g$ .

In a previous report by Fukao et al., it has been reported that the fragility decreases slightly with decreasing film thickness in thin films of PS on the basis of the combined results of dielectric relaxation spectroscopy and thermal expansion spectroscopy [23]. In a recent paper, a slight decrease in the fragility index from  $150$  to  $110$  was also observed using dielectric relaxation spectroscopy when the thickness was decreased from  $286$  nm to  $8.7$  nm [20]. The fragility index of PS-DR1 as a function of film thickness is shown in Table II. Although there is a large error, the observed results are qualitatively consistent with the previous results of unlabeled polystyrene.

The shapes of the dielectric loss and the distribution of relaxation times of the  $\alpha$ -process for thin films of PS-DR1 are shown in Figs. 8 and 9. The best fit parameters of the HN equation are listed for thin films of PS-DR1 with various film thickness at  $390$  K in Table I. It is illustrated in Figs. 8 and 9 that the distribution of the  $\alpha$ -relaxation times becomes broader with decreasing film thickness, which indicates that the thickness dependence of the distribution of the  $\alpha$ -relaxation times in PS-DR1 is the same as that of unlabeled PS. The broadening of the distribution of the  $\alpha$ -relaxation times with decreasing film thickness may result from a region at the upper Al-polymer interface with dynamics different from bulk dynamics. This hypothesis will be tested in a forthcoming paper [45]. We note that the distribution of PS-DR1 is narrower than that of unlabeled PS at a fixed thickness:  $\beta_{KWW} = 0.53$  for PS-DR1 with  $d = 360$  nm and  $\beta_{KWW} = 0.435$  for unlabeled PS with  $d = 408$  nm [17]. This may be related to the fact that the rotational reori-

entation dynamics of the DR1, which are coupled with the  $\alpha$ -process, are observed by dielectric relaxation spectroscopy.

Figure 6 we shows that there is a decrease in the strength of the  $\alpha$ -relaxation process with decreasing film thickness;  $\Delta\epsilon$  changes from 2.14 to 0.33 with decreasing film thickness from 360 nm to 19 nm. This thickness dependence of  $\Delta\epsilon$  is commonly observed in thin films of other polymeric systems such polystyrene, poly(methyl methacrylate), poly(vinyl acetate) and so on [18, 24]. In a previous report by Fukao et al., a simple model for the decrease in  $\Delta\epsilon$  in thin films was proposed and can be applied to thin films of PS labeled with DR1. In the model, it is assumed that there is a motional unit in which  $n$  dipole motions move or rotate cooperatively. In this case  $\Delta\epsilon$  is given by the following relation:

$$\Delta\epsilon = \frac{N\mu^2}{3k_B T}, \quad (8)$$

where  $N$  is the number of the motional units and is given by  $N_0 = N \times n$ , and  $\mu$  is the total strength of dipole moments included in a unit and is given by  $\mu = n\mu_0$ . Here,  $\mu_0$  is the strength of a single dipole moment attached to polymer chains,  $N_0$  is the total number of dipole moments in the system and it is assumed that there is no correlation between the motional units. Using  $N_0$  and  $\mu_0$ , we can rewrite Eq.(9) as follows:

$$\Delta\epsilon = n \frac{N_0\mu_0^2}{3k_B T}. \quad (9)$$

Therefore, if the number of dipole moments within the motional unit is decreased with decreasing film thickness, the decrease in  $\Delta\epsilon$  in thinner films can be accounted for. The idea of a decrease in the number of dipole moments moving cooperatively is consistent with that based on the existence of a cooperatively rearranging region (CRR) [3].

In supported ultrathin films of unlabeled PS, it has been reported that there is an additional relaxation process ( $\alpha_l$ -process) in addition to the  $\alpha$ -process [17, 20]. The  $\alpha_l$ -process is located at a lower temperature than that of the  $\alpha$ -process. This process was assigned to relaxation dynamics of the surface region in PS films, and has an Arrhenius type of temperature dependence with an activation energy of 71 kJ/mol [20]. A recent study investigating the relaxation processes of thin supported polystyrene films using dielectric spectroscopy also observed an additional relaxation process below  $T_g$  with an Arrhenius temperature dependence [46]. The activation energy of the additional process was 15-25 kJ/mol. However, the additional process was attributed to a simple or primitive dynamical process that acts as a precursor to the glass transition in ultrathin free standing films. In the present study, an  $\alpha_l$ -process is observed in ultrathin PS-DR1 films ( $d < 20$  nm) at temperatures lower than that of the  $\alpha$ -process, as shown in Fig. 11. From the investigation in Fig. 11, it is found that the  $\alpha_l$ -process of thin films of PS-DR1 can also be described by an Arrhenius type of activation process with the activation energy

$U = 68 \pm 3$  kJ/mol, which agrees very well with the value reported for the unlabeled PS [20]. At present, we cannot provide an unambiguous answer as to whether the additional relaxation process observed in the current study results from interfacial effects or a simple or primitive dynamical process. Studies are currently underway to determine whether or not it is an interfacial effect.

Here, it should be noted that the DR1 chromophore covalently attached to the main chain in PS-DR1 is a bulky group. Therefore, there is a possibility that the local structure of the amorphous PS chains deviates from that of the unlabeled PS and its deviation affects the dynamics of the polymer chains observed by dielectric relaxation spectroscopy. However, we believe that such deviation, if any, has almost no effect on the segmental motions of PS-DR1, because the  $\alpha$ -dynamics and its thickness dependence are consistent with those of unlabeled PS, as shown in our study. In addition, previous studies conducted using DR1 as the dye either doped or covalently attached to the polymer yielded average  $\alpha$ -relaxation times in agreement with those determined using other techniques.

## VI. SUMMARY

We investigated the glass transition temperature and relaxation dynamics of the  $\alpha$ -process of thin films of polystyrene labeled with a dye DR1 using dielectric relaxation measurements. The results can be summarized as follows:

1. The dielectric strength of DR1-labeled polystyrene is approximately 65 times as large as that of unlabeled polystyrene above the glass transition, while there is almost no difference between them below the glass transition.
2. The  $T_g$  of DR1-labeled polystyrene can be determined well as a crossover temperature at which the temperature coefficient of the electric capacitance changes from the value of the glassy state to that of the liquid state. The  $T_g$  thus obtained decreases with decreasing film thickness in a manner similar to that of unlabeled polystyrene thin films.
3. As for the dielectric relaxation spectrum of the DR1-labeled polystyrene, the  $\alpha$ -relaxation time becomes smaller and the distribution of the  $\alpha$ -relaxation times becomes broader, as thickness decreases.

These results show that there is a distinct contrast between the relaxation strength of the  $\alpha$ -process of PS-DR1 and that of the unlabeled PS and that thin films of DR1-labeled polystyrene are a suitable system for investigating confinement effects of the glass transition dynamics using dielectric relaxation spectroscopy. Therefore, we expect that we will be able to observe the dynamics of the  $\alpha$ -process only from the labeled

layer in a multi-layer system of PS-DR1 and unlabeled PS, and to obtain information on the dynamics of the  $\alpha$ -process at any position normal to the film surface. We will report the results on such position dependent measurements of the  $\alpha$ -dynamics in the near future [45].

### Acknowledgements

This work was supported by the NSF-MRSEC Program at Northwestern University (Grants DMR-0076097

and DMR-0520513), a Grant-in-Aid for Scientific Research (B) (No.16340122) from Japan Society for the Promotion of Science, a DFI fellowship (R.D.P.) and a NSF EASPI fellowship (R.D.P.).

- 
- [1] B. Frick, M. Koza, R. Zorn (Editors), Proceedings of the 2nd International Workshop on Dynamics in Confinement, Euro. Phys. J. **E12**, (2003).
- [2] Proceedings of the 4th International Discussion Meeting on Relaxations in Complex Systems, J. Non-Cryst. Solids, **307-310** (2002).
- [3] G. Adam and J.H. Gibbs, J. Chem. Phys. **43**, 139 (1965).
- [4] J. Schüller, Yu. B. Mel'nichenko, R. Richert, and E.W. Fischer, Phys. Rev. Lett. **73**, 2224 (1994).
- [5] M. Arndt, R. Stannarius, H. Groothues, E. Hempel, and F. Kremer, Phys. Rev. Lett. **79**, 2077 (1997).
- [6] J.L. Keddie, R.A.L. Jones, and R.A. Cory, Europhys. Lett., **27**, 59 (1994).
- [7] J.L. Keddie and R.A.L. Jones, Faraday Discuss. **98**, 219 (1994).
- [8] G.B. DeMaggio, W.E. Frieze, D.W. Gidley, Ming Zhu, H.A. Hristov, and A.F. Yee, Phys. Rev. Lett. **78**, 1524 (1997).
- [9] W.E. Wallace, J.H. van Zanten, and W.L. Wu, Phys. Rev. **E52**, R3329 (1995).
- [10] B. Jerome and J. Commandeur, Nature, **386**, 589 (1997).
- [11] M. Yu. Efremov, E. A. Olson, M. Zhang, Z. Zhang, and L. H. Allen Phys. Rev. Lett. **91**, 085703 (2003)
- [12] V. Lupascu, H. Huth, C. Schick, M. Wübbenhorst, Thermochimica Acta **432**, 222 (2005).
- [13] J.A. Forrest, K. Dalnoki-Veress, J.R. Stevens, and J.R. Dutcher, Phys. Rev. Lett. **77**, 2002 (1996).
- [14] J.A. Forrest, K. Dalnoki-Veress, and J.R. Dutcher, Phys. Rev. **E56**, 5705 (1997).
- [15] J.A. Forrest, J. Mattsson, Phys. Rev. **E61**, R53 (2000).
- [16] K. Fukao and Y. Miyamoto, Europhys. Lett. **46**, 649 (1999).
- [17] K. Fukao and Y. Miyamoto, Phys. Rev. **E61**, 1743 (2000).
- [18] L. Hartmann, W. Gorbatschow, J. Hauwede, F. Kremer, Eur. Phys. J. **E8** 145 (2002).
- [19] A. Serghei, F. Kremer, Phys. Rev. Lett. **91**, 165702 (2003).
- [20] V. Lupascu, S.J. Picken, M. Wübbenhorst, J. Non-Cryst. Solids, **352**, 5594 (2006).
- [21] K. Akabori, K. Tanaka, T. Nagamura, A. Takahara, T. Kajiyama, Macromolecules, **38**, 9735 (2005).
- [22] D.B. Hall, J.C. Hooker, J.M. Torkelson, Macromolecules, **30**, 667 (1997).
- [23] K. Fukao and Y. Miyamoto, Phys. Rev. **E64**, 011803 (2001).
- [24] K. Fukao, S. Uno, Y. Miyamoto, A. Hoshino, and H. Miyaji, Phys. Rev. **E64**, 051807 (2001).
- [25] K. Fukao, Euro. Phys. J. **E 12**, 119 (2003).
- [26] C.J. Ellison, J.M. Torkelson, Nature Mater. **2**, 695 (2003).
- [27] P. J. Hains, G. Williams, Polymer, **16**, 725 (1975).
- [28] M. S. Dionisio, J. J. Moura-Ramos, and G. Williams, Polymer, **34**, 4105 (1993).
- [29] M. S. Dionisio, J. J. Moura-Ramos, and G. Williams, Polymer, **35**, 1705 (1994).
- [30] O. van den Berg, M. Wübbenhorst, S. J. Picken, and W. F. Jager, J. Non-Cryst. Solids, **351**, 2694 (2005).
- [31] O. van den Berg, W. G. F. Sengers, W. F. Jager, S. J. Picken, and M. Wübbenhorst, Macromolecules, **37**, 2460 (2004).
- [32] W. Huang and R. Richert, J. Chem. Phys., **124**, 164510 (2006).
- [33] G. F. L. Ferreira, M. T. Figueiredo, S. N. Fedosov, and J. A. Giacometti, J. of Physics D, Applied Physics, **31**, 2051 (1998).
- [34] A. Dhinojwala, J. C. Hooker, J. M. Torkelson, J. Non-Cryst. Solids **172**, 286 (1994).
- [35] L-T. Cheng et al., J. Phys. Chem., **95**, 10631 (1991).
- [36] A. Dhinojwala, G. K. Wong, J. M. Torkelson, J. Chem. Phys. **100** 6046 (1994).
- [37] Y. Miyamoto, Polymer **25**, 63 (1984).
- [38] S. Havriliak and S. Negami, Polymer **8**, 161 (1967).
- [39] H. Vogel, Phys. Z. **22**, 645 (1921); G.S. Fulcher, J. Am. Ceram. Soc. **8**, 339, 789 (1925).
- [40] R. Böhmer and C.A. Angell, Phys. Rev. **B45** 10091 (1992).
- [41] P. Papadopoulos, D. Peristeraki, G. Floudas, G. Koutalas, N. Hadjichristidis, Macromolecules, **37**, 8116 (2004).
- [42] M.L. Williams, R.E. Landel, J.D. Ferry, J. Am. Chem. Soc. **77**, 3701 (1955).
- [43] C. Bauer, R. Böhmer, S. Moreno-Flores, R. Richert, H. Sillescu, and D. Neher, Phys. Rev. **E61**, 1755 (2000).
- [44] F. Alvarez, A. Alegria, J. Colmenero, Phys. Rev. **B44** 7306 (1991).
- [45] R.D. Priestley, L.J. Broadbelt, K. Fukao, J.M. Torkelson, in preparation.
- [46] C. Svanberg, Macromolecules, **40**, 312 (2007).